THE JOURNAL OF PHYSICAL CHEMISTRY Letters

Letter

pubs.acs.org/JPCL

Comparing Charge Transport in Oligonucleotides: RNA:DNA Hybrids and DNA Duplexes

Yuanhui Li,[†] Juan M. Artés,[†,∥] Jianqing Qi,[‡] Ian A. Morelan,[§,⊥] Paul Feldstein,[§] M. P. Anantram,[‡] and Joshua Hihath*[,†]

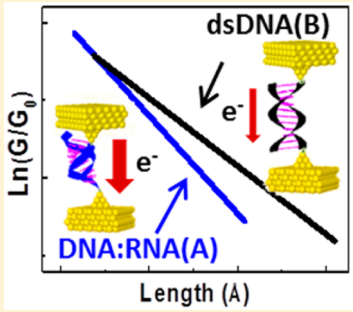
[†]Electrical and Computer Engineering Department, University of California Davis, Davis, California 95616, United States

[‡]Department of Electrical Engineering, University of Washington, Seattle, Washington 98195, United States

[§]Department of Plant Pathology, University of California Davis, Davis, California 95616, United States

Supporting Information

ABSTRACT: Understanding the electronic properties of oligonucleotide systems is important for applications in nanotechnology, biology, and sensing systems. Here the charge-transport properties of guanine-rich RNA:DNA hybrids are compared to double-stranded DNA (dsDNA) duplexes with identical sequences. The conductance of the RNA:DNA hybrids is ∼10 times higher than the equivalent dsDNA, and conformational differences are determined to be the primary reason for this difference. The conductance of the RNA:DNA hybrids is also found to decrease more rapidly than dsDNA when the length is increased. Ab initio electronic structure and Green's function-based density of states calculations demonstrate that these differences arise because the energy levels are more spatially distributed in the RNA:DNA hybrid but that the number of accessible hopping sites is smaller. These combination results indicate that a simple hopping model that treats each individual guanine as a hopping site is insufficient to explain both a higher conductance and β value for RNA:DNA hybrids, and larger delocalization lengths must be considered.



DNA has long been espoused as the molecule of life,[1] and given its unique structural and self-assembly properties it is often proclaimed as an important material for nanotechnology.[2−4] Because of this substantial promise, a great deal of research has focused on both its mechanical[5−7] and electrical[8−13] properties. Meanwhile, our understanding of the biological importance of RNA has also continuously increased in recent decades. It is now known that RNA plays a pivotal role in gene expression and regulating biochemical reactions within the cell,[14] and it is the messenger between DNA and ribosomes and proteins.[15,16] Recently, it has also been determined that RNA is even involved in the immunological responses of many organisms.[17,18] To fulfill these roles, RNA can assemble with complementary DNA strands to form RNA:DNA hybrids that are integral to many biological processes, including DNA replication,[19−21] transcription during gene expression,[22] and reverse transcription.[23,24] Although chemically similar, single-stranded (ss) RNA differs from ssDNA in a couple of important ways. First, in RNA, uracil bases replace the thymine bases found in DNA, and second the backbones are different with RNA having a ribose group instead of the deoxyribose that is present in DNA. Despite these differences, RNA:DNA hybrids are capable of forming a double helix, with the base pairs (bp) arranged in a π stack,[25,26] in a way analogous to dsDNA. dsDNA has been well-documented to allow long-range charge transport through the π stack under certain conditions.[26,27] Therefore, it is expected that RNA:DNA hybrids will also transport charge;[28] however, the structure of the RNA:DNA helix is significantly different from the common B-form dsDNA structure.[29] The RNA:DNA hybrid is predominantly in the A-form, while dsDNA is typically in the B-form under physiological conditions.[30,31] As such, the electronic overlap between the π orbitals in the bases will be different, which could lead to substantial differences in the charge-transport properties of RNA:DNA hybrids compared with those of dsDNA. Given both the biological significance of RNA and RNA:DNA hybrids, the similarities in structure, and self-assembly properties of these systems to DNA, it is important to explore the electronic properties of these systems for both molecular electronics and biosensor applications.

Driven by the importance of this vital molecule, various experimental and theoretical approaches have been employed to understand charge transfer in RNA:DNA using photochemical[31−33] and electrochemical[34,35] measurements. Alternatively, in this work, we directly study the conductance properties of RNA:DNA hybrids and compare them with identical dsDNA duplexes at the single-molecule level using the scanning tunneling microscope (STM)-break junction technique in a buffered solution.[36] This technique has been extensively applied to study charge transport through organic and biological molecules.[37−41] It provides the advantages of being able to work in an aqueous, controllable environment, and collecting thousands of conductance measurements in a

Received: April 7, 2016
Accepted: May 4, 2016
Published: May 4, 2016

ACS Publications © 2016 American Chemical Society

DOI: 10.1021/acs.jpclett.6b00749
J. Phys. Chem. Lett. 2016, 7, 1888−1894

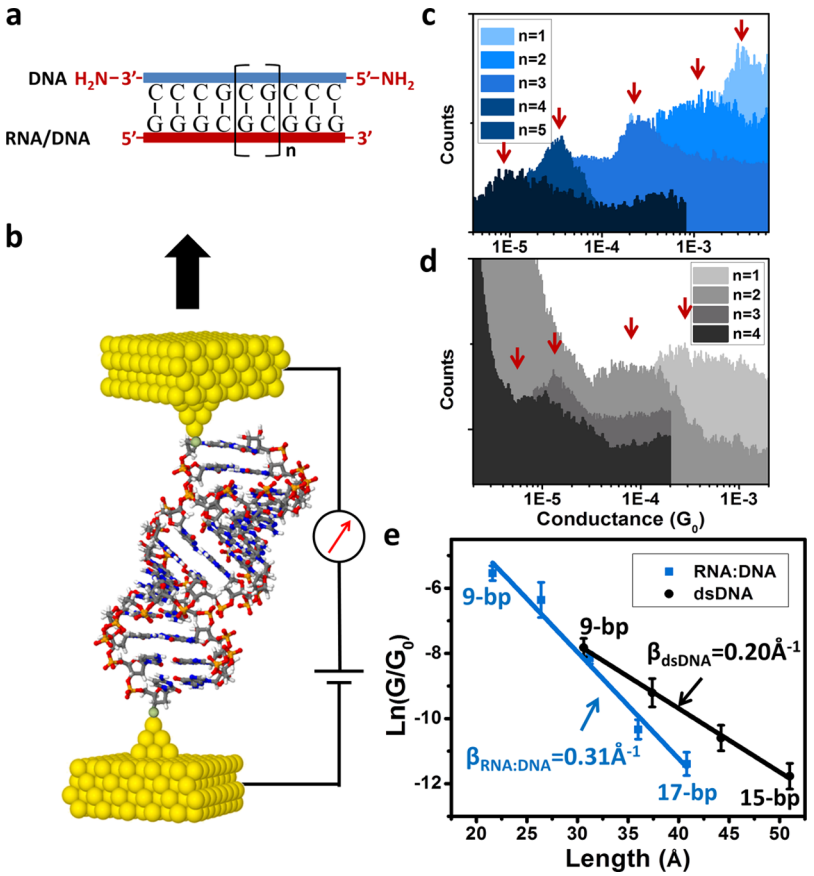


Figure 1. Length dependence of RNA:DNA and dsDNA conductance. (a) Schematic of the guanine-rich sequences used for length dependence studies for RNA:DNA and dsDNA. (b) Idealized schematic of the experimental setup showing a 15-bp RNA:DNA molecule bound between two gold electrodes with amine linkers (shown as green spheres). (c,d) Conductance histograms for each of the RNA:DNA and dsDNA molecules studied, respectively. The arrows indicate the conductance peak for each sequence. (Note that histograms are offset vertically and the tails of some histograms are cut for clarity. Please see Figure S2 for the completed histograms). (e) Natural logarithm of conductance versus length for RNA:DNA (blue squares) and B-form dsDNA (black circles). Error bars are full widths at half-maximum (fwhm) for the conductance peaks.

relatively short time period. As such, this technique enables the statistical analysis of the most probable conductance values for a single-molecule junction in a known environment. In the past decade, this technique has been used to obtain reproducible conductance values for biomolecules such as dsDNA,[13,42−47] peptides,[48,49] and proteins.[50,51]

We present a systematic study of the charge-transport properties of individual RNA:DNA and dsDNA duplexes in a sodium phosphate buffer solution using the STM-break junction technique.[52] We study a series of G:C-only RNA:DNA sequences (GGG-C$(GC)_n$-GGG, with n = 1−5) and the identical dsDNA sequences with n = 1−4 and extract their length-dependent exponential decay constants (β values). We find that the conductance of each RNA:DNA sequence is approximately 1 order of magnitude higher than that of the B-form dsDNA with the same sequence and demonstrate that the conformational differences between the two duplexes play a pivotal role in the transport properties. We use circular dichroism (CD) spectroscopy to confirm that the conformations of the two oligonucleotides are different (A form and B form for RNA:DNA and dsDNA, respectively). Furthermore, by inducing the A-form in dsDNA using a 75% ethanol solution we are able to increase the conductance of the dsDNA to a similar level as the RNA:DNA hybrid, thus confirming that the transport differences between the two duplexes are primarily due to changes in the structure rather than the composition.[53]

To understand the differences in the structural and electrical properties of both oligonucleotides we use ab initio electronic structure calculations to conclude that differences in absolute conductance and β value between RNA:DNA and dsDNA are primarily due to their structural differences. These results demonstrate that electronic-transport studies are capable of extracting relevant structural and biological information from a hybrid oligonucleotide duplex and thus open the door for further studies on conductance-based RNA detection.

To examine the charge-transport properties of RNA:DNA hybrids, we have explored the length dependence of the conductance of these molecules and also measured the conductance of the equivalent dsDNA duplexes for comparison. The conductance of a tunneling junction can be represented by $G = G_c e^{-\beta L}$, where G_c is the contact conductance, β is the tunneling decay constant, and L is the distance between the electrodes. The value of the decay constant, β, is often used as a figure of merit to provide insights into the charge-transport properties of the system. A large β value indicates a substantial decrease in conductance with increasing length and is typically used as an evidence of a single-step tunneling process.[54] Alternatively, a small β value means that the conductance decreases less strongly with length and is often used as an indication of a hopping mechanism.[13] Thus, we performed break-junction measurements on the series of RNA:DNA duplexes previously described, with n = 1−5, and

DOI: 10.1021/acs.jpclett.6b00749
J. Phys. Chem. Lett. 2016, 7, 1888−1894

on the identical dsDNA sequences with n = 1−4 (see Figure 1a). We modify both the 5′ and 3′ ends of the DNA strand with amine linkers to ensure a good binding between the RNA:DNA hybrid and the gold electrodes used in the STM[38,55] (see SI). Figure 1b illustrates a schematic of the measurement system with a 15-bp DNA:RNA molecule linked between the gold tip electrode and the gold substrate. With this break junction technique, thousands of individual conductance measurements can be obtained rapidly for statistical analysis, allowing the most probable conductance of a single molecule to be determined by adding all of the traces with steps to a conductance histogram. The conductance histograms for each of these RNA:DNA (9−17 bp) and dsDNA (9−15 bp) duplexes are shown in Figure 1c,d, respectively. The conductance histograms for each duplex show a single, pronounced peak. From these plots, two observations can be readily made. First, these plots allow direct comparison between the RNA:DNA hybrids and the dsDNA, and it is clear that for each specific sequence the conductance of the RNA:DNA hybrid is about 10 times higher than the equivalent dsDNA duplex. Second, it is apparent that the conductance peak shifts to lower conductance values with increasing lengths. By plotting the natural log of conductance versus molecular length (Figure 1e), it is possible to obtain the β values. This process yields a β value of 0.31 Å^{-1} for RNA:DNA hybrids (Figure 1e, blue) and 0.20 Å^{-1} for dsDNA duplexes (Figure 1e, black). Although these β values are different, both are consistent with a hopping-based transport mechanism,[56] which has previously been reported for GC-rich dsDNA sequences.[31] Additional control experiments performed on solutions containing only the single-stranded DNA with amine linkers, only single-stranded RNA, and RNA:DNA hybrids without linkers did not result in obvious peaks in the experimentally accessible conductance range (Figure S1).

As previously mentioned, although the sequences are identical for both duplexes, the conductance of each RNA:DNA hybrid is higher than the respective dsDNA duplex. This difference could be due to either conformational or chemical differences. The chemical difference between the two molecules is the addition of a hydroxyl group on the ribose in the case of the RNA strand; however, the charge transport is expected to be through the π system,[27,57] and the bases of RNA:DNA and dsDNA are the same in these sequences (no uracil is included). Thus, this chemical difference is not expected to significantly affect the charge-transport properties of these systems. Therefore, we focus on the structural differences between the two molecules instead of the chemical difference. RNA:DNA hybrids are well known to be stabilized in the A-form,[58] while dsDNA is expected to adopt the B-form conformation in buffered solutions.[30,35] To verify this point, we performed CD spectroscopy on both of the duplexes in a 100 mM sodium phosphate buffer solution (Figure 2a). The primary indicator of the A-form conformation is the appearance of an intense negative peak at 210 nm,[58] and this peak is clearly visible in the RNA:DNA hybrid (Figure 2a, blue). We expect this structural difference to be the dominant cause of the conductance differences between these two duplexes, as recently demonstrated for A-form and B-form dsDNA.[53]

To test this hypothesis, we also examined the CD spectrum and conductance of the 11-bp dsDNA duplex in the A-form conformation by solubilizing it in a 75% ethanol solution (v/v) to compare with both the RNA:DNA hybrid and the B-form dsDNA. Figure 2a (green) shows the CD spectrum of the 11-bp dsDNA in ethanol solution. Although there are some

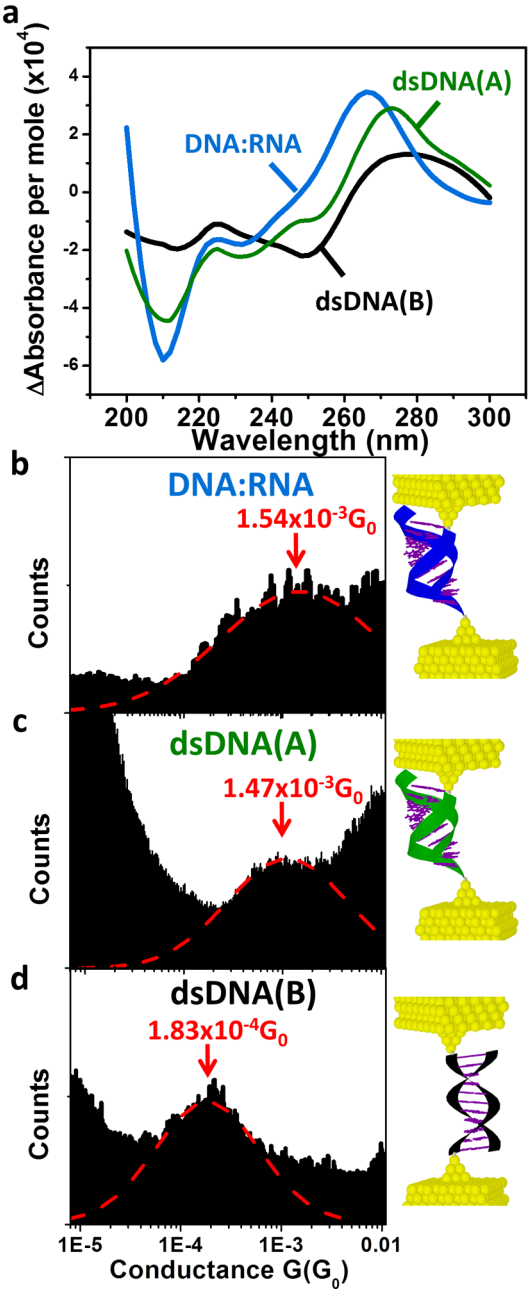


Figure 2. Structure induced conductance differences. (a) CD spectra of a RNA:DNA hybrid (blue), A-form dsDNA (green), and B-form dsDNA (black) duplexes. (b−d) Conductance histograms of a GGG-CGCGC-GGG sequence in the case of an RNA:DNA hybrid, A-form dsDNA, and B-form dsDNA, respectively. Red curves are the Gaussian fitting of the conductance peaks. The right schematics correspond to the junctions formed with the different conformations for each molecule.

differences between the 11-bp DNA duplex in ethanol and the RNA:DNA hybrid (Figure 2a, blue), which can be attributed to the effect of ethanol on the absorption properties,[30,59] there is a clear negative peak at 210 nm, indicating the stabilization of the A-form conformation in this solution. By comparing individual conductance histograms of RNA:DNA hybrids, A-form dsDNA, and B-form dsDNA, as shown in Figure 2b−d, we find that the conductance of 11-bp RNA:DNA hybrid is very similar to the conductance of A-form dsDNA and that both of these are ∼10 times higher than B-form dsDNA, thus verifying that the

DOI: 10.1021/acs.jpclett.6b00749
J. Phys. Chem. Lett. 2016, 7, 1888−1894

primary difference in the transport properties of these molecules is structural rather than chemical.

Interestingly, both the conductance and the β value of RNA:DNA are larger than B-form dsDNA. To understand how the structural differences between these duplexes relate to these effects, we have performed a series of electronic structure calculation using first-principles calculations (Gaussian 09 software package with the B3LYP/6-31G(d,p) functional and basis set) coupled to Green's function techniques[60] to examine the changes in the energy levels and determine the density of states (DoS) for these molecules.

We have recently demonstrated that A-form DNA is higher in conductance than B-form DNA due to an increased spatial distribution of energy levels in the A-form, coupled to an increase in the DoS around the highest occupied molecular orbital (HOMO) level in this configuration.[53] Given the similarities in structure and conductance values between A-form DNA and RNA:DNA hybrids, we hypothesize that a similar effect causes the conductance difference seen here. To examine this possibility, in Figure 3a,b we present the HOMO isosurface

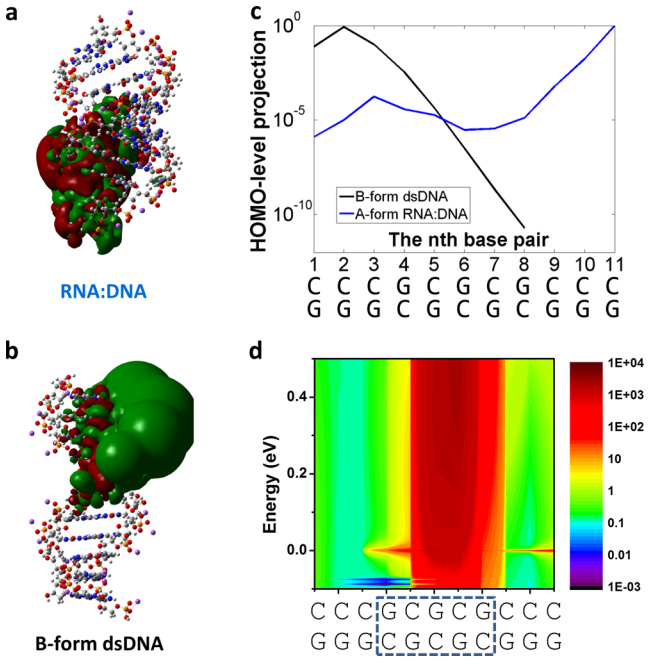


Figure 3. Results from charge-transport simulations of 11-bp RNA:DNA and B-form dsDNA. (a,b) 3D isosurface of the HOMO orbital (isovalue = 2×10^{-5}) on the oligonucleotide structures for RNA:DNA and B-form dsDNA. (c) Projection of the HOMO level onto each of the base pairs in the A-form RNA:DNA (blue solid line) and B-form dsDNA (black solid line). There is no contribution to the HOMO level for the 9th to 11th base pairs in dsDNA. (d) 2D representation of the ratio of the total density of states (DoS) along the molecule between RNA:DNA hybrids and B-form dsDNA for an energy ranging from HOMO−0.1 to 0.5 eV above HOMO level.

plots of the 11-bp sequence for both the RNA:DNA hybrids and the B-form dsDNA with an isovalue of 2×10^{-5}. At this value the HOMO level is distributed over ∼70% of the length of the RNA:DNA hybrid and over only ∼50% of the length of the B-form dsDNA. This effect can be seen more quantitatively by examining the projection of the HOMO level onto each of the base pairs in the duplex (Figure 3c). Additionally, as shown in Figure S4, the HOMO levels are distributed through approximately the same number of bp's for the entire dsDNA family studied (from the first to eighth bp), but for RNA:DNA series they are distributed through the entire molecule, regardless of length. These results show that all of the base pairs contribute to the HOMO level in the RNA:DNA case, while in the B-form contribution drops off rapidly after the first G triplet. This indicates a higher delocalization of the HOMO orbital in the RNA:DNA case.

This difference in the distribution and contribution of the HOMO level to the electronic structure can be visualized by examining the differences in the DoS in the two systems. Figure 3d shows the ratio of the 2D DoS of the RNA:DNA hybrid to the B-form dsDNA near HOMO level along the entire length of the 11-bp sequences. For these plots the HOMO level of each molecule is set to zero energy, and the DoS is plotted as both a function of both energy (ordinate) and molecular length (abscissa). From these plots it is apparent that in GGG triplet regions on each end the DoS are similar in both cases (ratio is close to 1); however, in the central bridge region (alternating GC sequence in the dashed box), it is clear that near the HOMO level the DoS in the RNA:DNA hybrids is much larger (as much as 10^4 times greater) than the DoS for dsDNA in this region. Along with the isosurface plots (Figure 3a,b) and the projected HOMO distribution (Figure 3c), these results suggest that for a given number of bp's, charge should transport more efficiently (have a higher conductance) in the RNA:DNA hybrid case (A-form) than in the B-form dsDNA case. This result is consistent across the entire range of molecules studied (Figure S3).

Next, we turn our attention to the question of why the conductance decreases more rapidly (larger β value) in the RNA:DNA hybrid than in the B-form DNA case. As previously noted, the low β values in both cases are consistent with a hopping transport mechanism, and in DNA it has often been assumed that because guanines have the lowest oxidation potential each guanine in the system will act as an individual hopping site;[61] however, it has also been noted that a charge carrier could be delocalized over more than one base and that the transport may include both incoherent and coherent components.[28,62−64] In the discussion above, we demonstrated that the energy levels can be distributed over several base pairs in each duplex, indicating that it is insufficient to treat each guanine individually as a hopping site for either of these systems. As such, in these molecules, the number of hopping sites is likely not simply the number of base pairs or guanines in the system but instead depends on both the spatial and energy distribution of the system's energy levels. This fact in turn indicates that the charge carriers may require fewer total hops to transport across the entire molecule. In this case, the number of hopping sites may be different for each of the oligonucleotide duplexes, a detail that will have important impacts on the transport properties and the β value.

To examine this possibility more closely and determine how it relates to the difference in the β values between the two systems, we examine 2D DoS plots in Figure 4 for all RNA:DNA and dsDNA sequences with a coupling term (Γ = 100 meV) between the molecule and both gold electrodes. These plots display both the spatial and energy distribution of the states, and the z-color scale indicates the density of states at each position. Here we focus on the energy range below the HOMO level because the transport is expected to be dominated by hole transport.[65−67] The bright horizontal stripes represent the spatial distribution of each of the Kohn−Sham energy levels for the molecular system, and again the HOMO

DOI: 10.1021/acs.jpclett.6b00749
J. Phys. Chem. Lett. 2016, 7, 1888−1894

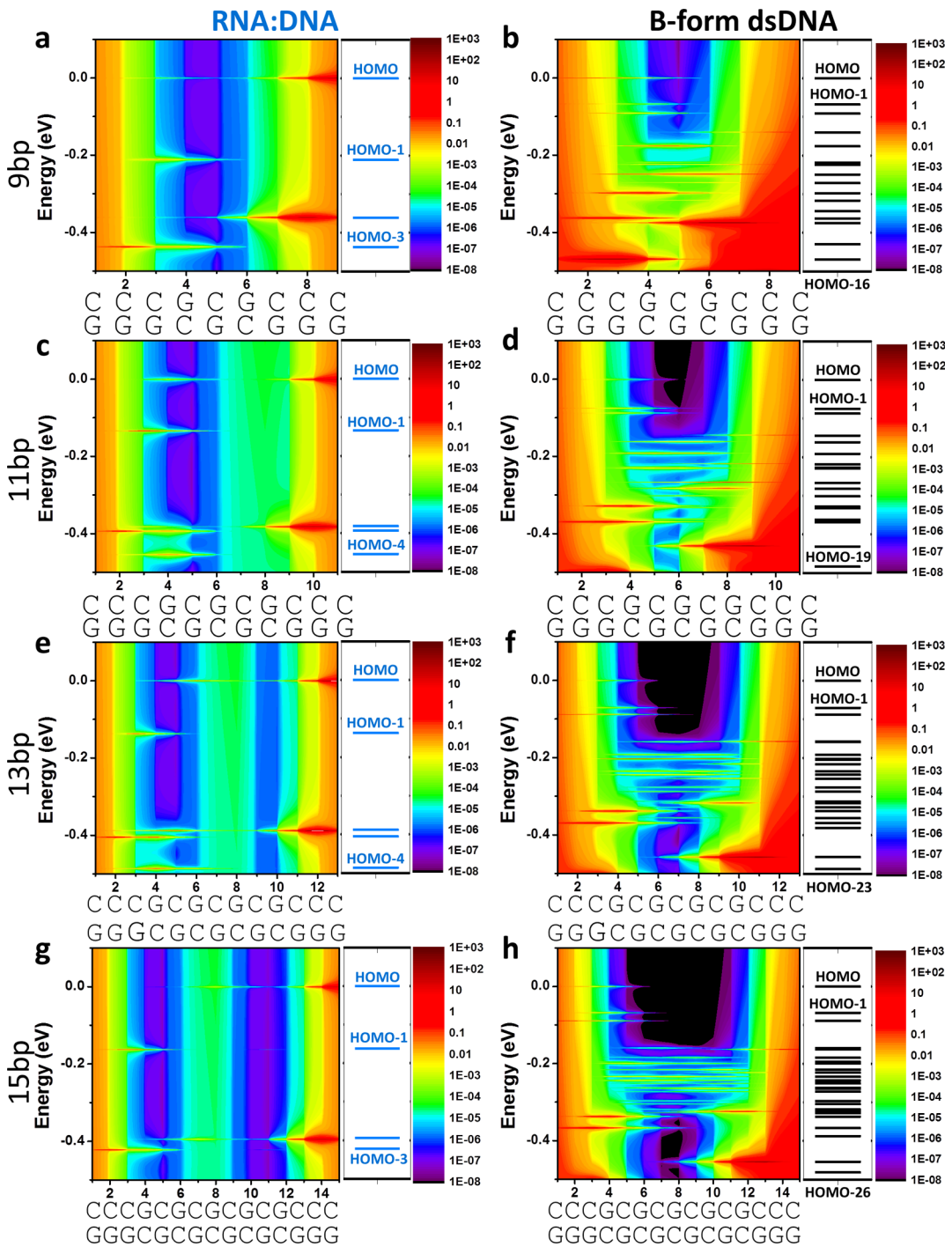


Figure 4. 2D total DoS along the molecule of (a) 9-bp, (c) 11-bp, (e) 13-bp, and (g) 15-bp RNA:DNA hybrid and (b) 9-bp, (d) 11-bp, (f) 13-bp, and (h) 15-bp B-form dsDNA, respectively, for an energy ranging from HOMO−0.5 to 0.1 eV above HOMO level. The 1D energy-level plots are shown on the right side of each plot. (HOMO = 0 eV in all cases). In this energy window, there are many more energy levels for dsDNA than in RNA:DNA for each length.

level is taken as zero energy in each case. In these plots, each of the energy levels (molecular orbitals) is distributed over several base pairs, in agreement with the isoplots in Figure 3a,b. The lines next to each of the 2D DoS colormaps indicate the values of the calculated energy levels and show that the levels are more distributed in energy for the RNA:DNA hybrids. This separation will result in weaker coupling between the levels than in the B-form DNA case.[6] Additionally, because the energy levels in the RNA:DNA case are more sparse (separated by several k_BT) suggests that there are few energy levels close to the HOMO-level that are accessible as hopping sites. Furthermore, as the length increases, the number of potential hopping sites does not significantly increase throughout the RNA:DNA series (Figure 4a,c,e,g). Alternatively, in the B-form DNA case, there are many potential hopping sites (energy levels), and this number increases with increasing length (Figure 4b,d,f,h). The smaller number of accessible hopping sites, coupled to the larger energy separation between them, is

DOI: 10.1021/acs.jpclett.6b00749
J. Phys. Chem. Lett. 2016, 7, 1888−1894

expected to result in a larger β value in the RNA:DNA hybrid case.

In summary, we have measured the conductance of individual RNA:DNA hybrids using the STM break junction technique in aqueous solution. We show that the conductance of these G:C-rich RNA:DNA hybrids is approximately 1 order of magnitude higher than the equivalent dsDNA sequence. We attribute this to their conformational differences rather than chemical differences. We demonstrate that the conformations of RNA:DNA and B-form dsDNA are significantly different using CD spectroscopy and confirm this effect as the origin of the conductance difference by comparing the RNA:DNA hybrid to the A-form DNA duplex. Length-dependent conductance studies suggest that the charge-transport mechanism in both oligonucleotides is dominated by hopping. These observations are accounted for by using ab initio electronic structure calculations coupled to Green's Function-based DoS calculations, which reveal that simple nearest-neighbor hopping between guanine bases is insufficient to accurately treat the transport behavior. The theoretical calculations of projected HOMO distributions show that the HOMO level is more distributed along the molecules in RNA:DNA duplexes, which suggests a higher conductance than dsDNA. The 2D DoS calculations also provide additional insights into both the spatial and energy distribution of the molecular orbitals. From these plots it is clear that fewer hopping sites are available in the RNA:DNA duplex case and thus result in a higher distance decay factor as the length increases. Given the importance of RNA in biological systems, this electrical measurement of RNA could open the door to single-molecule sensors with applications in the fundamental biomedical research and genetic diseases diagnosis.

■ ASSOCIATED CONTENT

Supporting Information

The Supporting Information is available free of charge on the ACS Publications website at DOI: 10.1021/acs.jpclett.6b00749.

Control experiments, complete conductance histograms of RNA:DNA and dsDNA, 2D ratio of DoS calculations, projection of HOMO level calculations; experimental details of sample preparation and measurements, and computational simulation procedure. (PDF)

■ AUTHOR INFORMATION

Corresponding Author

*E-mail: jhihath@ucdavis.edu.

Present Addresses

[‖]J.M.A.: Faculty of Sciences, Vrije Universiteit, 1081 HV Amsterdam, The Netherlands.

[⊥]I.A.M.: Department of Integrative Biology, Oregon State University, Corvallis, Oregon 97331, United States.

Notes

The authors declare no competing financial interest.

■ ACKNOWLEDGMENTS

Y.L., J.M.A., I.A.M., P.F., and J.H. acknowledge the University of California, Davis RISE program and the National Science Foundation (ECCS-1231915). J.Q. and M.P.A. acknowledge support from the National Science Foundation under Grant No. 102781.

■ REFERENCES

(1) Frank-Kamenetskiĭ, M. D. *Unraveling DNA: The Most Important Molecule of Life*; Addison-Wesley: Reading, MA, 1997

(2) Pinheiro, A. V.; Han, D.; Shih, W. M.; Yan, H. Challenges and Opportunities for Structural DNA Nanotechnology. *Nat. Nanotechnol.* **2011**, *6*, 763−772.

(3) Seeman, N. C. DNA in a Material World. *Nature* **2003**, *421*, 427−431.

(4) Stoltenberg, R. M.; Woolley, A. T. DNA-Templated Nanowire Fabrication. *Biomed. Microdevices* **2004**, *6*, 105−111.

(5) Smith, S. B.; Finzi, L.; Bustamante, C. Direct Mechanical Measurements of the Elasticity of Single DNA Molecules by Using Magnetic Beads. *Science* **1992**, *258*, 1122−1126.

(6) Gaub, H. E.; Rief, M.; Clausen-Schaumann, H. Sequence-Dependent Mechanics of Single DNA Molecules. *Nat. Struct. Biol.* **1999**, *6*, 346−349.

(7) Bustamante, C.; Smith, S. B.; Liphardt, J.; Smith, D. Single Molecule Studies of DNA Mechanics. *Curr. Opin. Struct. Biol.* **2000**, *10*, 279−285.

(8) De Pablo, P. J.; Moreno-Herrero, F.; Colchero, J.; Gómez Herrero, J.; Herrero, P.; Baró, A. M.; Ordejón, P.; Soler, J. M.; Artacho, E. Absence of Dc-Conductivity in λ-DNA. *Phys. Rev. Lett.* **2000**, *85*, 4992−4995.

(9) Storm, A. J.; Van Noort, J.; De Vries, S.; Dekker, C. Insulating Behavior for DNA Molecules between Nanoelectrodes at the 100 Nm Length Scale. *Appl. Phys. Lett.* **2001**, *79*, 3881−3883.

(10) Porath, D.; Bezryadin, A.; de Vries, S.; Dekker, C. Direct Measurement of Electrical Transport through DNA Molecules. *Nature* **2000**, *403*, 635−638.

(11) Yoo, K. H.; Ha, D. H.; Lee, J. O.; Park, J. W.; Kim, J.; Kim, J. J.; Lee, H. Y.; Kawai, T.; Choi, H. Y. Electrical Conduction through poly(dA)-poly(dT) and poly(dG)-poly(dC) DNA Molecules. *Phys. Rev. Lett.* **2001**, *87*, 198102.

(12) Fink, H. W.; Schönenberger, C. Electrical Conduction through DNA Molecules. *Nature* **1999**, *398*, 407−410.

(13) Xu, B.; Zhang, P.; Li, X.; Tao, N. Direct Conductance Measurement of Single DNA Molecules in Aqueous Solution. *Nano Lett.* **2004**, *4*, 1105−1108.

(14) McCaffrey, A. P.; Meuse, L.; Pham, T. T. T.; Conklin, D. S.; Hannon, G. J.; Kay, M. A. Gene Expression: RNA Interference in Adult Mice. *Nature* **2002**, *418*, 38−39.

(15) Lehman, I. R.; Bessman, M. J.; Simms, E. S.; Kornberg, A. Enzymatic Synthesis of Deoxyribonucleic Acid. *J. Biol. Chem.* **1958**, *233*, 163−170.

(16) Crick, F. H. C.; Barnett, L.; Brenner, S.; Watts-Tobin, R. J. General Nature of the Genetic Code for Proteins. *Nature* **1961**, *192*, 1227−1232.

(17) Pennisi, E. The CRISPR Craze. *Science* **2013**, *341*, 833−836.

(18) Barrangou, R. Cas9 Targeting and the CRISPR Revolution. *Science* **2014**, *344*, 707−708.

(19) Bibb, M. J.; Van Etten, R. A.; Wright, C. T.; Walberg, M. W.; Clayton, D. A. Sequence and Gene Organization of Mouse Mitochondrial DNA. *Cell* **1981**, *26*, 167−180.

(20) Kornberg, A.; Baker, T. A. *DNA Replication*; W.H. Freeman: San Francisco, 1980.

(21) Lark, K. G. Evidence for the Direct Involvement of RNA in the Initiation DNA Replication in Escherichia Coli 15T. *J. Mol. Biol.* **1972**, *64*, 47−60.

(22) Agris, P. F. Decoding the Genome: A Modified View. *Nucleic Acids Res.* **2004**, *32*, 223−238.

(23) Telesnitsky, A.; Goff, S. P. *Reverse Transcriptase and the Generation of Retroviral DNA*; Cold Spring Harbor Laboratory Press: Cold Spring Harbor, NY, 1997

(24) Summers, J.; Mason, W. S. Replication of the Genome of a Hepatitis B–like Virus by Reverse Transcription of an RNA Intermediate. *Cell* **1982**, *29*, 403−415.

(25) Lin, J. C.; Singh, R. R. P.; Cox, D. L. Theoretical Study of DNA Damage Recognition via Electron Transfer from the [4Fe-4S] Complex of MutY. *Biophys. J.* **2008**, *95*, 3259−3268.

DOI: 10.1021/acs.jpclett.6b00749
J. Phys. Chem. Lett. 2016, 7, 1888−1894

(26) Endres, R. G.; Cox, D. L.; Singh, R. R. P. Colloquium: The Quest for High-Conductance DNA. *Rev. Mod. Phys.* **2004**, *76*, 195−214.
(27) Berlin, Y. A.; Voityuk, A. A.; Ratner, M. A. DNA Base Pair Stacks with High Electric Conductance: A Systematic Structural Search. *ACS Nano* **2012**, *6*, 8216−8225.
(28) Li, Y.; Artés, J. M.; Hihath, J. Long-Range Charge Transport in Adenine-Stacked RNA:DNA Hybrids. *Small* **2016**, *12*, 432−437.
(29) Egli, M.; Usman, N.; Rich, A. Conformational Influence of the Ribose 2′ -Hydroxyl Group: Crystal Structures of DNA-RNA Chimeric Duplexes. *Biochemistry* **1993**, *32*, 3221−3237.
(30) Kypr, J.; Kejnovská, I.; Renčiuk, D.; Vorlíčková, M. Circular Dichroism and Conformational Polymorphism of DNA. *Nucleic Acids Res.* **2009**, *37*, 1713−1725.
(31) O'Neil, M. A.; Barton, J. K. 2-Aminopurine: A Probe of Structural Dynamics and Charge Transfer in DNA and DNA:RNA Hybrids. *J. Am. Chem. Soc.* **2002**, *124*, 13053−13066.
(32) Sartor, V.; Henderson, P. T.; Schuster, G. B. Radical Cation Transport and Reaction in RNA/DNA Hybrid Duplexes: Effect of Global Structure on Reactivity. *J. Am. Chem. Soc.* **1999**, *121*, 11027−11033.
(33) Kratochvílová, I.; Vala, M.; Weiter, M.; Špérová, M.; Schneider, B.; Páv, O.; Šebera, J.; Rosenberg, I.; Sychrovský, V. Charge Transfer through DNA/DNA Duplexes and DNA/RNA Hybrids: Complex Theoretical and Experimental Studies. *Biophys. Chem.* **2013**, *180*, 127−134.
(34) Gorodetsky, A. A.; Buzzeo, M. C.; Barton, J. K. DNA-Mediated Electrochemistry. *Bioconjugate Chem.* **2008**, *19*, 2285−2296.
(35) Boon, E. M.; Barton, J. K. DNA Electrochemistry as a Probe of Base Pair Stacking in A-, B-, and Z-Form DNA. *Bioconjugate Chem.* **2003**, *14*, 1140−1147.
(36) Reed, M. A.; Zhou, C.; Muller, C. J.; Burgin, T. P.; Tour, J. M. Conductance of a Molecular Junction. *Science* **1997**, *278*, 252−254.
(37) Guo, S.; Zhou, G.; Tao, N. Single Molecule Conductance, Thermopower, and Transition Voltage. *Nano Lett.* **2013**, *13*, 4326−4332.
(38) Chen, F.; Li, X.; Hihath, J.; Huang, Z.; Tao, N. Effect of Anchoring Groups on Single-Molecule Conductance: Comparative Study of Thiol-, Amine-, and Carboxylic-Acid-Terminated Molecules. *J. Am. Chem. Soc.* **2006**, *128*, 15874−15881.
(39) Venkataraman, L.; Klare, J. E.; Nuckolls, C.; Hybertsen, M. S.; Steigerwald, M. L. Dependence of Single-Molecule Junction Conductance on Molecular Conformation. *Nature* **2006**, *442*, 904−907.
(40) Quinn, J. R.; Foss, F. W.; Venkataraman, L.; Hybertsen, M. S.; Breslow, R. Single-Molecule Junction Conductance through Diaminoacenes. *J. Am. Chem. Soc.* **2007**, *129*, 6714−6715.
(41) Fatemi, V.; Kamenetska, M.; Neaton, J. B.; Venkataraman, L. Environmental Control of Single-Molecule Junction Transport. *Nano Lett.* **2011**, *11*, 1988−1992.
(42) Hihath, J.; Guo, S.; Zhang, P.; Tao, N. Effects of Cytosine Methylation on DNA Charge Transport. *J. Phys.: Condens. Matter* **2012**, *24*, 164204.
(43) Yu, H.; Shan, X.; Wang, S.; Chen, H.; Tao, N. Plasmonic Imaging and Detection of Single DNA Molecules. *ACS Nano* **2014**, *8*, 3427−3433.
(44) Hihath, J.; Chen, F.; Zhang, P.; Tao, N. Thermal and Electrochemical Gate Effects on DNA Conductance. *J. Phys.: Condens. Matter* **2007**, *19*, 215202.
(45) Hihath, J.; Xu, B.; Zhang, P.; Tao, N. Study of Single-Nucleotide Polymorphisms by Means of Electrical Conductance Measurements. *Proc. Natl. Acad. Sci. U. S. A.* **2005**, *102*, 16979−16983.
(46) van Zalinge, H.; Schiffrin, D. J.; Bates, A. D.; Haiss, W.; Ulstrup, J.; Nichols, R. J. Single-Molecule Conductance Measurements of Single- and Double-Stranded DNA Oligonucleotides. *ChemPhysChem* **2006**, *7*, 94−98.
(47) Kratochvílová, I.; Todorciuc, T.; Král, K.; Nemec, H.; Buncek, M.; Šebera, J.; Záliš, S.; Vokácová, Z.; Sychrovský, V.; Bednárová, L.; et al. Charge Transport in DNA Oligonucleotides with Various Base-Pairing Patterns. *J. Phys. Chem. B* **2010**, *114*, 5196−5205.
(48) Xiao, X.; Xu, B.; Tao, N. Conductance Titration of Single-Peptide Molecules. *J. Am. Chem. Soc.* **2004**, *126*, 5370−5371.
(49) Xiao, X.; Xu, B.; Tao, N. Changes in the Conductance of Single Peptide Molecules upon Metal-Ion Binding. *Angew. Chem., Int. Ed.* **2004**, *43*, 6148−6152.
(50) Artés, J. M.; Díez-Pérez, I.; Gorostiza, P. Transistor-like Behavior of Single Metalloprotein Junctions. *Nano Lett.* **2012**, *12*, 2679−2684.
(51) Della Pia, E. A.; Elliott, M.; Jones, D. D.; MacDonald, J. E. Orientation-Dependent Electron Transport in a Single Redox Protein. *ACS Nano* **2012**, *6*, 355−361.
(52) Xu, B.; Tao, N. J. Measurement of Single-Molecule Resistance by Repeated Formation of Molecular Junctions. *Science* **2003**, *301*, 1221−1223.
(53) Artés, J. M.; Li, Y.; Qi, J.; Anantram, M. P.; Hihath, J. Conformational Gating of DNA Conductance. *Nat. Commun.* **2015**, *6*.887010.1038/ncomms9870
(54) Segal, D.; Nitzan, A.; Davis, W. B.; Wasielewski, M. R.; Ratner, M. a. Electron Transfer Rates in Bridged Molecular Systems 2. A Steady-State Analysis of Coherent Tunneling and Thermal Transitions. *J. Phys. Chem. B* **2000**, *104*, 3817−3829.
(55) Venkataraman, L.; Klare, J. E.; Tam, I. W.; Nuckolls, C.; Hybertsen, M. S.; Steigerwald, M. L. Single-Molecule Circuits with Well-Defined Molecular Conductance. *Nano Lett.* **2006**, *6*, 458−462.
(56) Gray, H. B.; Winkler, J. R. Long-Range Electron Transfer. *Proc. Natl. Acad. Sci. U. S. A.* **2005**, *102*, 3534−3539.
(57) Wagenknecht, H. A. *Charge Transfer in DNA*; Wiley-VCH: Weinheim, Germany, 2005; p 369.
(58) Lesnik, E. A.; Freier, S. M. Relative Thermodynamic Stability of DNA, RNA, and DNA:RNA Hybrid Duplexes: Relationship with Base Composition and Structure. *Biochemistry* **1995**, *34*, 10807−10815.
(59) Ivanov, V. I.; Minchenkova, L. E.; Minyat, E. E.; Frank-Kamenetskii, M. D.; Schyolkina, A. K. The B to A Transition of DNA in Solution. *J. Mol. Biol.* **1974**, *87*, 817−833.
(60) Frisch, M. J.; Trucks, G. W.; Schlegel, H. B.; Scuseria, G. E.; Robb, M. A.; Cheeseman, J. R.; Scalmani, G.; Barone, V.; Mennucci, B.; Petersson, G. A.; et al. *Gaussian 09*, Revision D.1; Gaussian: Wallingford, CT, 2009.
(61) Seidel, C. A. M.; Schulz, A.; Sauer, M. H. M. Nucleobase-Specific Quenching of Fluorescent Dyes. 1. Nucleobase One-Electron Redox Potentials and Their Correlation with Static and Dynamic Quenching Efficiencies. *J. Phys. Chem.* **1996**, *100*, 5541−5553.
(62) Xiang, L.; Palma, J. L.; Bruot, C.; Mujica, V.; Ratner, M. a.; Tao, N. Intermediate Tunnelling−hopping Regime in DNA Charge Transport. *Nat. Chem.* **2015**, *7*, 221−226.
(63) O'Neil, M. A.; Barton, J. K. DNA Charge Transport: Conformationally Gated Hopping through Stacked Domains. *J. Am. Chem. Soc.* **2004**, *126*, 11471−11483.
(64) Kendrick, T.; Giese, B. Charge Transfer through DNA Triggered by Site Selective Charge Injection into Adenine. *Chem. Commun.* **2002**, *18*, 2016−2017.
(65) Meggers, E.; Michel-Beyerle, M. E.; Giese, B. Sequence Dependent Long Range Hole Transport in DNA. *J. Am. Chem. Soc.* **1998**, *120*, 12950−12955.
(66) Voityuk, A. A.; Jortner, J.; Bixon, M.; Rösch, N. Energetics of Hole Transfer in DNA. *Chem. Phys. Lett.* **2000**, *324*, 430−434.
(67) Giese, B. Long-Distance Electron Transfer through DNA. *Annu. Rev. Biochem.* **2002**, *71*, 51−70.

DOI: 10.1021/acs.jpclett.6b00749
J. Phys. Chem. Lett. 2016, 7, 1888−1894